

Molecular dynamics simulation of ionic mobility. I. Alkali metal cations in water at 25 °C

Song Hi Lee

Department of Chemistry, Kyung Sung University, Pusan 608-736, Korea

Jayendran C. Rasaiah

Department of Chemistry, University of Maine, Orono, Maine 04469

(Received 12 April 1994; accepted 29 June 1994)

We describe a series of molecular dynamics simulations performed on model cation-water systems at 25 °C representing the behavior of Li^+ , Na^+ , K^+ , Rb^+ , and Cs^+ in an electric field of 1.0 V/nm and in its absence. The TIP4P model was used for water and TIPS potentials were adapted for the ion-water interactions. The structure of the surrounding water molecules around the cations was found to be independent of the applied electric field. Some of the dynamic properties, such as the velocity and force autocorrelation functions of the cations, are also field independent. However, the mean-square displacements of the cations, their average drift velocities, and the distances traveled by them are field dependent. The mobilities of the cations calculated directly from the drift velocity or the distance traveled by the ion are in good agreement with each other and they are in satisfactory agreement with the mobilities determined from the mean-square displacement and the velocity autocorrelation function in the absence of the field. They also show the same trends with ionic radii that are observed experimentally; the magnitudes are, however, smaller than the experimental values in real water by almost a factor of 2. It is found that the water molecules in the first solvation shell around the small Li^+ ion are stuck to the ion and move with it as an entity for about 190 ps, while the water molecules around the Na^+ ion remain for 35 ps, and those around the large cations stay for 8–11 ps before significant exchange with the surroundings occurs. The picture emerging from this analysis is that of a solvated cation whose mobility is determined by its size as well as the static and dynamic properties of its solvation sheath and the surrounding water. The classical solventberg model describes the mobility of Li^+ ions in water adequately but not those of the other ions.

I. INTRODUCTION

One of the classical areas of study in physical chemistry is the mobility of ions at infinite dilution and their dependence on ion size and the properties of the solvent.¹ The simplest continuum model predicts that the ionic mobility is inversely proportional to the radius of the ion, as required by Stokes' law.² Experimental observations, however, indicate that the ionic mobilities in aqueous solution do not decrease monotonically with increasing radius as seen in Fig. 1 which shows the ionic conductance at infinite dilution, λ^0 , as a function of the crystallographic radius R . In 1920, Max Born³ proposed that the continuum model could be modified to understand deviations from Stokes' law by considering the dielectric friction of the solvent on the ion. In this case, the solvent is treated as a viscous dielectric continuum polarized by the ion. Ion transport disturbs the equilibrium polarization of the solvent, and the relaxation of the ensuing nonequilibrium polarization dissipates energy making the friction on the ion larger than it would be if the solvent was a viscous medium without dielectric properties.

The dielectric friction effect of the solvent on an ion was further developed by Fuoss,⁴ Boyd,⁵ and Zwanzig.⁶ In Zwanzig's theory, the total friction

$$\zeta = 4\pi\eta R(1 + \theta\gamma). \quad (1)$$

Here $\theta=3/2$, R is the ion radius, η is the solvent viscosity, $\gamma=(K/R)^4$, and

$$K^4 = \frac{q_i^2(\epsilon_0 - \epsilon_\infty)\tau_D}{16\pi\eta\epsilon_0^2} \quad (2)$$

in which q_i is the charge on the ion, ϵ_0 and ϵ_∞ are the static and high frequency dielectric constants respectively, and τ_D is the Debye relaxation time. K has the units of length and is nearly 1.5 Å for monovalent ions in water at 25 °C. The first and second terms in Eq. (1) are the viscous drag $\zeta_S = 4\pi\eta R$ (assuming slip boundary conditions) and the drag $\zeta_D = 6\pi\eta R\gamma$ due to dielectric friction respectively. The ratio $\zeta_D/\zeta_S = \alpha$ is about 7.6 and 0.72, respectively, for Na^+ and Cl^- ions in water at 25 °C, using radii of 0.95 and 1.81 Å, respectively, for these ions. This implies a relatively large dielectric friction effect on Na^+ ions and a much smaller one for Cl^- ions.

The mobility $u = q_i/\zeta$, and it follows from Eq. (1) that the limiting molar ionic conductance $\lambda^0 = uF$ is given by

$$\lambda^0 = AR^3/(C + R^4), \quad (3)$$

where $A = Fq_i/(6\pi\eta)$, F is the Faraday and C is a constant determined by the viscosity, dielectric relaxation time, and the static and high frequency dielectric constants of the solvent. Frank¹ observed that Eq. (3), labeled $B-F-B-Z$ in Fig. 1, has a maximum $(\lambda^0)_m = (3^{3/4}/4)AC^{-1/4}$ at $(R)_m = (3C)^{1/4}$ which is nearly 2.34 Å for monovalent ions in water at 25 °C. This is close to the observed maxima in the ionic conductances, at 1.7 and 2.1 Å, respectively, of the alkali metal ions and the halides. However, $(\lambda^0)_m$ calculated

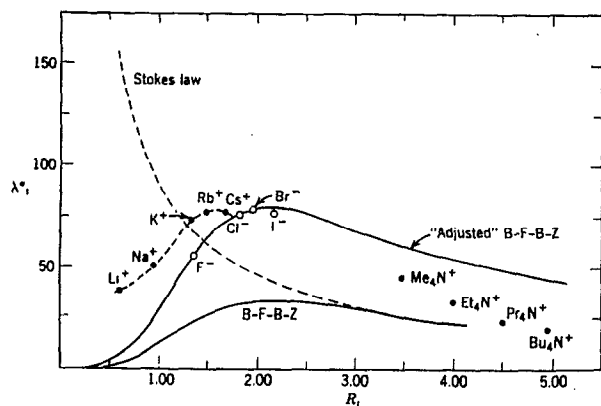


FIG. 1. Ionic conductance at 25 °C of simple monovalent ions at infinite dilution in water plotted vs the crystallographic radius. The curve *B-F-B-Z* is the dielectric friction theory developed successively by Born, Fuoss, Boyd, and Zwanzig and the "adjusted" *B-F-B-Z* curve is obtained by adjustment of the parameters to get exact agreement for the Br^- ion (see Ref. 1 from which figure is adapted).

from Eq. (3), using the bulk viscosity of water, is much smaller than the measured conductances near the maximum. A near perfect fit for the halides was obtained by treating A and C as adjustable parameters on the grounds that it is the local viscosity rather than the bulk value that should be used in Eq. (3). This is the "adjusted" *B-F-B-Z* curve in Fig. 1. Note, however, that the conductances of the alkali metal ions and the halides lie on different curves.

The theory of Hubbard and Onsager^{7,8} (HO) is perhaps the most sophisticated and complete of the continuum dielectric theories of ionic mobility developed so far. They proposed a set of electrohydrodynamic equations that satisfy a symmetry principle first enunciated by Born³ but incompletely applied by him. Hubbard and Onsager argued that rigid body motion of an inhomogeneously polarized dielectric should lead to no dissipation. The HO theory determines the dielectric friction as a function of R and K , renamed the Hubbard-Onsager radius R_{HO} ($=K$). When $\gamma < 1$, the friction ζ can be represented as a convergent series in powers of $\gamma = (R_{\text{HO}}/R)^4$. The leading term in this expansion, assuming slip boundary conditions, is given by Eq. (1) with $\theta = 4/15$. This implies a smaller dielectric friction effect than that predicted by Zwanzig's theory. For example, $\gamma \approx 0.17$ and 0.63 , respectively, for Na^+ and K^+ ions in water at 25 °C when R is the crystallographic radius.

Hubbard and Kayser⁹ (HK) extended the HO theory by considering the effect of the rotational viscosity η_R of the solvent. The limit $\eta_R \rightarrow \infty$ corresponds to the original Hubbard-Onsager (HO) theory, while the limit $\eta_R \rightarrow 0$ leads to Eq. (1) with $\theta = 8/45$ implying a further lowering of the dielectric friction. Another development is also due to Hubbard and Kayser,^{10,11} who analyzed the effect of the dielectric saturation on ion mobility for which only numerical results are available. Although the HO and HK theories lead to numerical differences and a smaller dielectric friction in the HK theory, they both predict finite friction for point charges ($R \rightarrow 0$).

Recently, Nakahara and co-workers¹² found that the HO

theory was successful in explaining the temperature and pressure dependence of friction for small ions like Li^+ and Na^+ but failed to do so in the case of large ions like Cs^+ . Paradoxically, the dielectric continuum model does not consider details of the static and dynamic properties of the inner solvent shells of small ions which we find, in this study, to be the dominant factors that determine the mobility of these ions. The model also incorrectly assumes a continuous medium up to the surface of the ion, and it further supposes that the time in which the solvent polarization force on the ion relaxes is the macroscopic relaxation time.

To explain the puzzle of the low mobilities at infinite dilution of small ions, it is necessary to take account of the ion-solvent interaction at a molecular level. The oldest of these is the classical "solventberg" picture invoked by chemists in which the ion moves with its first solvation sheath rigidly bound to it, making it effectively larger than the bare ion. While this might be approximately correct for small ions, the picture is oversimplified since nuclear magnetic resonance (NMR) studies¹³ indicate molecular motion within the first shell of univalent ions.

Wolynes¹⁴ proposed a molecular theory of limiting ionic mobility that incorporates the solventberg picture and the dielectric friction model as limiting cases. The theory, developed with many simplifying assumptions, begins quite generally with the separation of the forces acting on the ion into a rapidly varying part, due to the hard collisions of solvent molecules with the ion, and a more slowly varying part arising from the softer attractive forces between the ion and the solvent molecules. The ionic friction coefficient ζ , related as usual to the fluctuations in the random forces $\mathbf{F}(t)$ exerted on the ion, splits into components arising from the correlations of the hard repulsive (H) and soft attractive (S) parts of the force. Thus

$$\zeta = 1/(3kT) \int_0^\infty \langle \mathbf{F}(0)\mathbf{F}(t) \rangle dt = \zeta^{HH} + \zeta^{SH} + \zeta^{HS} + \zeta^{SS}. \quad (4)$$

Here ζ^{HH} is the contribution to the drag from the hard collisions with the solvent. It is identified with Stokes law assuming that the hydrodynamic radius equals the ion radius.¹⁴ A second approximation ignores the correlations between the soft and hard components, namely ζ^{SH} and ζ^{HS} . The physical interpretation of these terms implies that a hard collision event leads later to a fluctuation in the attractive force on the ion. The theory then focuses on the time dependence of the fluctuations of the soft forces, i.e., ζ^{SS} . These fluctuations, analyzed approximately as arising from the molecular motion of solvent molecules, provide an expression for the drag coefficient

$$\zeta = \zeta_0 + (1/3kT) \langle F_s^2 \rangle \tau_F. \quad (5)$$

Here $\zeta_0 = \zeta^{HH}$ is the viscous drag given by Stokes' law, while $\langle F_s^2 \rangle$ is the static mean-square fluctuation in the soft forces and τ_F is their characteristic decay time. The determination of τ_F is the key to the theory. It is related to the self-correlation function of the time derivative of the soft force, for which Colonomos and Wolynes,¹⁴ proposed a simple factorization approximation which lead to numerical estimates

of ionic mobilities. Their results for cations in water, especially for Na^+ ion, are in good agreement with the experiment. These theoretical developments have been reviewed in the literature.¹⁵

Molecular dynamics simulations of ion mobility take an entirely different approach to these problems. They were first performed by Ciccotti and Jacucci¹⁶ who applied a direct external electric field on an ion in a Lennard-Jones solvent and calculated the mobility of a positive ion in liquid argon in excellent agreement with experiment. Gosling and Singer¹⁷ studied the dynamics of a single univalent ion in a diatomic solvent with fractional charges on the atoms that correspond to a molecular dipole moment of 4.32 D and Pollock and Alder¹⁸ investigated ion transport in a monatomic, polarizable solvent.

Many other studies of the mobilities of aqueous ionic solutions by computer simulation have appeared.^{19–25} Impey, Madden, and McDonald²¹ carried out a molecular dynamics study of Li^+ , Na^+ , K^+ , F^- , and Cl^- ions using the MCY model of water to obtain the static structure around the ions and the residence time of water molecules in the first coordination shell around the ion. They defined a dynamic hydration number for the ion as the ratio of two residence times, one for the ion and the other for bulk water. Wilson, Pohorille, and Pratt²² calculated the velocity autocorrelation function of Na^+ in MCY water and determined its friction coefficient from the force autocorrelation function of the ion. They tested the accuracy of the assumption of Brownian motion of the ions that is the basis of many models of ion mobility. Berkowitz and Wan²³ used molecular dynamics simulations to calculate the limiting ionic mobilities for Na^+ and Cl^- ions in TIP4P water. They found that the memory kernels for the generalized Langevin equation from the velocity autocorrelation function of the mobile ion and the autocorrelation function of the force exerted on the stationary ion are in good agreement. However, the simulations do not confirm one of the major assumptions of Wolynes' theory¹⁴ that the correlations between the soft and hard parts, namely ζ^{SH} and ζ^{HS} , are small. Reddy and Berkowitz²⁴ investigated the temperature dependence of the self-diffusion coefficient of the Li^+ , Cs^+ , and Cl^- ions in water by molecular dynamics simulation. More recently, Rose and Benjamin²⁵ calculated the ionic mobilities of Na^+ and Cl^- in their study of the adsorption of the ions at the charged water–platinum interface. The calculated mobilities at low electric fields underestimated the experimental value,²⁶ but agreed with the experimental facts²⁷ that the ionic mobilities at infinite dilution are approximately independent of the external field. The mobilities calculated at large fields on the other hand overestimated the experimental values.

Apart from these studies of ion mobilities, we also note that recent molecular dynamics simulations of ion solvation in a Stockmayer fluid and in water^{28–30} imply that solvent relaxation occurs with two time scales: a short time behavior described by a Gaussian function followed by a longer exponential time decay modulated by oscillatory behavior.

It appears that none of the theoretical descriptions of ion mobility is entirely satisfactory and computer simulations of this are fragmented and inconclusive. A renewed investiga-

tion of this problem, using simulation as a guide to theory, would be helpful. In this paper, we discuss results of molecular dynamics simulations of a cation and 215 water molecules. We focus our attention on the most relevant static and dynamic properties of the solvation shells around the ion. The cations selected are models of the alkali metal ions Li^+ , Na^+ , K^+ , Rb^+ , and Cs^+ in aqueous solutions at infinite dilution and at 25 °C. The main purpose of our study is to investigate the dependence of cation mobilities on their radii, and especially to investigate the puzzle of the low mobilities of small cations. The mobility of large cations is also incompletely understood and needs careful study.

To mimic the real system between two electrodes, we apply an electric field that exerts a constant force acting on each particle in the system. The mobility is calculated directly from the drift velocity or the distance traveled by the ion. The magnitude of the electric field is chosen as 1.0 V/nm (10^9 V/m) which is the smallest value used by us in previous studies of the polarization dynamics of dipoles between charged plates³¹ and by Rose and Benjamin²⁵ in their studies of adsorption of ions near charged platinum–water surfaces. Apart from the paper by Rose and Benjamin on Na^+ and Cl^- , we know of no other studies that determine the mobility directly from data obtained in the presence of an electric field. We also calculate the mobilities from the diffusion coefficients in the absence of a field. The agreement between the two sets of calculations is satisfactory considering the difficulty in obtaining accurate statistics on a single ion. The dynamics of the hydration sheath around each ion is also investigated by computing the residence times of water near an ion. This is similar to earlier work described by Impey *et al.*²¹ on ions in MCY water. Stereoscopic pictures of the equilibrated hydration sheaths around lithium and cesium ions are also shown in this paper.

The paper is organized as follows. Section II contains a brief description of molecular models and molecular dynamics simulation methods followed by Sec. III which presents the results of our simulation results and Sec. IV where our conclusions are summarized.

II. MOLECULAR DYNAMICS SIMULATIONS

We treat the water molecules as rigid bodies with a monomer geometry and pair potential that corresponds to the well-known TIP4P model.³² Moreover, the interaction potentials between water and ion have the TIPS form^{33,34}

$$\phi_{iw} = 4\epsilon_{io} \left[\left(\frac{\sigma_{io}}{r_{io}} \right)^{12} - \left(\frac{\sigma_{io}}{r_{io}} \right)^6 \right] + \sum_{j \in w} \frac{q_i q_j}{r_{ij}}. \quad (6)$$

Here ϕ_{iw} is the interaction potential between an ion and water, ϵ_{io} and σ_{io} are Lennard-Jones parameters between oxygen on a water molecule and an ion i , q_j is the charge at site j in water, and q_i is the charge on ion i . In addition, r_{io} and r_{ij} are the distances between ion i and an oxygen site of a water molecule and between ion i and a charge site j in water.

Potential parameters for Li^+ – Na^+ , and Cs^+ –water interactions are from Refs. 33, 34, and 24. The parameters describing TIP4P water– K^+ and TIP4P water– Rb^+ are not

TABLE I. Ion water and water-water potential parameters. In the TIP4P model for water, the charges on H are at 0.9572 Å from the Lennard-Jones center at O. The negative charge is at site M located 0.15 Å away from O along the bisector of the HOH angle of 104.52°.

Ion/water	σ_{io} (Å)	ϵ_{io} (kJ/mol)	Charge (q)
Li ⁺	2.2068	4.1181	+1
Na ⁺	2.4647	3.6774	+1
K ⁺	2.7021	3.4964	+1
Rb ⁺	2.9394	3.4964	+1
Cs ⁺	3.1768	3.4964	+1
TIP4P	$\sigma_{oo}(A)$	$\epsilon_{oo}(kJ/mol)$	Charge (q)
O(H ₂ O)	3.1536	0.64873	
M(H ₂ O)			-1.04
H(H ₂ O)			+0.52

available in the literature; they were obtained from the potential energy curves of TIP4P water–Na⁺ and TIP4P water–Cs⁺ by interpolation. We assumed the σ_{io} 's for TIP4P water–K⁺ and TIP4P water–Rb⁺ correspond to one-third and two-thirds, respectively, of the difference between the values for TIP4P water–Cs⁺ and TIP4P water–Na⁺. We also assume that the ϵ_{io} 's for TIP4P water–K⁺ and TIP4P water–Rb⁺ are the same as that for TIP4P water–Cs⁺. These parameters are given in Table I and the potential curves of TIP4P water cations for the trigonal orientation³⁵ are shown in Fig. 2. The potentials were modified by the Steinhäuser switching function³⁶ which smoothly reduces the total energy from its value at $r=R_L$ to zero at $r=R_U$. For water–water and ion–water interactions we took $R_U=0.90$ nm and $R_L=0.95R_U$. An external electric field was applied in the z direction with the magnitude of 1.0 V/nm. The field causes the water molecules to rotate and the cation to drift in the direction of the field. However, as we will see, the magnitude of this field is small enough not to disturb the static and some

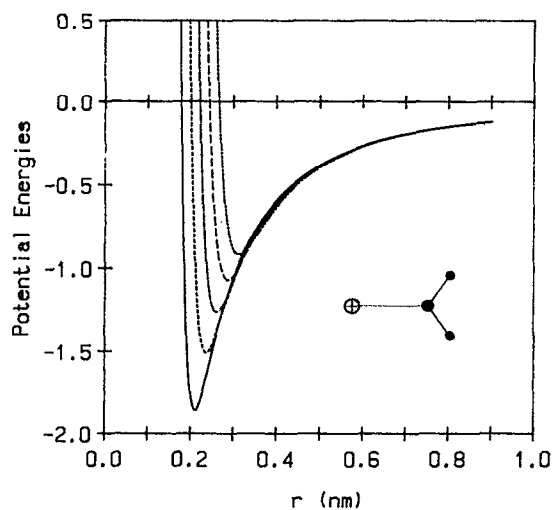


FIG. 2. Pair potentials of the cation-water interactions for the trigonal orientation of the TIP4P water molecule. (—) for Li⁺–water, (---) for Na⁺–water, (.....) for K⁺–water, (---) for Rb⁺–water, and (— · — · —) for Cs⁺–water.

of the dynamic properties of the system. The potential energy parameters that we assume may not be the optimum values that best mimic ion–water interactions in real systems, but that should not affect the main conclusions of our study.

We used Gaussian isokinetics^{37–39} to keep the temperature of the system constant and the quaternion formulation⁴⁰ of the equations of rotational motion about the center of mass of the TIP4P water molecules. For the integration over time, we adapted Gear's fifth-order predictor-corrector algorithm⁴¹ with a time step of 0.5×10^{-15} s (0.5 fs). In our canonical ensemble (NVT) molecular dynamics simulations, we initially equilibrated 216 water molecules at 298 K and 1 atm, and then replaced one of the water molecules by a cation. Further runs of at least 100 000 time steps each were needed for the cation–water system, with or without an electric field, to reach equilibrium. The equilibrium properties were then averaged over five blocks of 40 000 time steps (20 ps), for a total of 200 000 time steps (100 ps). The configurations of molecules were stored every 10 time steps for further analysis.

III. RESULTS AND DISCUSSION

In this section we analyze the results of our molecular dynamics simulations at 298 K; the principal static and dynamic properties are considered separately.

A. Static properties

The orientations of water molecules in the vicinity of the cation were determined from two orientational distribution functions in the first hydration shell whose radius is defined by the position of the first minimum in the cation–water radial distribution functions. In one, the probability $P(\theta)$ of observing a water dipole at an angle θ to the cation–oxygen vector was calculated and in the other, the probability $P(\phi)$ of observing the water OH vector at an angle ϕ to the cation–oxygen vector was determined. Figures 3 and 4 show these probabilities as functions of θ and ϕ , respectively. We also calculated the corresponding probability functions for water in the second shells of Li⁺ and Cs⁺ ions; they are displayed in the same figures.

Figure 3 shows that the most favorable orientation of a water dipole in the first shell is not parallel to the cation–oxygen vector but shifts from an angle of 22° to 52° with this vector as the radii of the cations increase from Li⁺ to Cs⁺. The distributions also become broader as the cation size increases. These changes are probably due to the competition between the strong cation–water electrostatic interaction and the interactions between the water molecules that include the tendency to maintain a hydrogen bonded network. Thus Fig. 3 also reflects the weakening of the cation–water interactions as the cation radius increases (see also Fig. 5).

The orientational distribution function $P(\phi)$ of Fig. 4 can also be interpreted similarly. Both angular distribution functions $P(\theta)$ and $P(\phi)$ are essentially unaltered (not shown) by an electric field of 1.0 V/nm. This implies that the applied field is not large enough to significantly perturb the orientation of water molecules in the first solvation shell.

The effect of the cation size on the structure of the sur

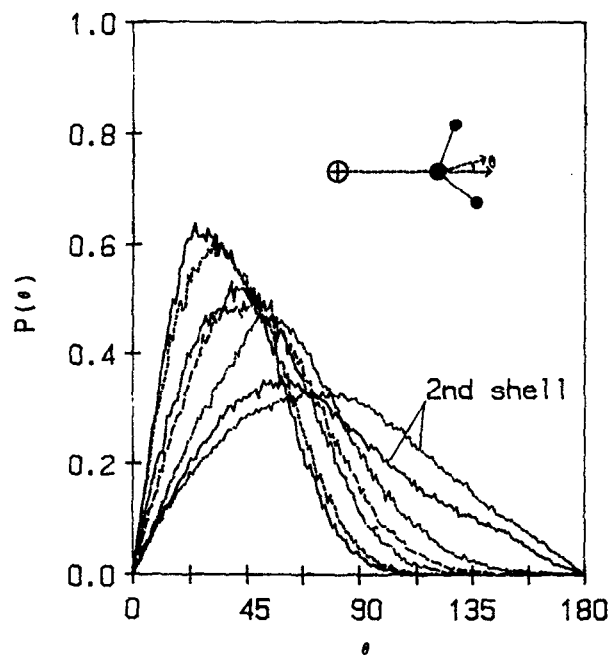


FIG. 3. Probability distribution functions for observing the cation-oxygen vector at an angle θ with a TIP4P water dipole in the first solvation shell of the cations Li^+ , Na^+ , K^+ , Rb^+ , and Cs^+ and in the second shell of solvent for only Li^+ and Cs^+ ions. The notation is the same as in Fig. 2.

rounding water is also apparent in Fig. 5, which shows the center of mass radial distribution functions $g_{iw}(r)$ of water molecules around different cations in the absence of an applied electric field. The height of the first peak diminishes

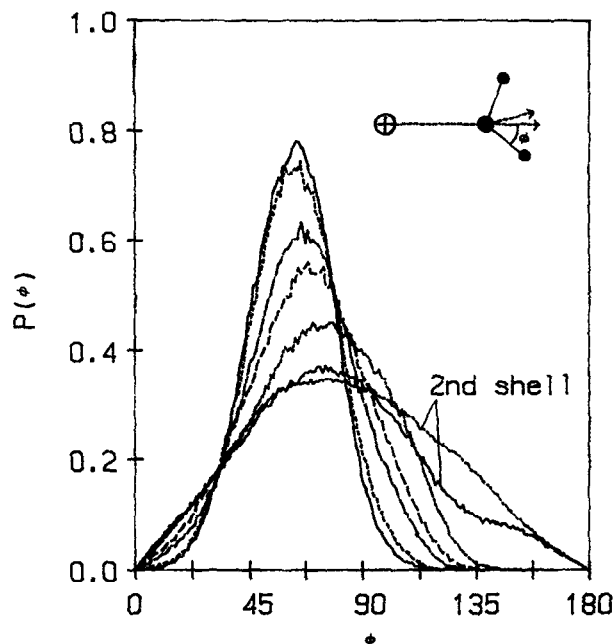


FIG. 4. Probability distribution functions for observing the cation-oxygen vector at an angle ϕ with a TIP4P water OH vector in the first solvation shell of the cations Li^+ , Na^+ , K^+ , Rb^+ , and Cs^+ and in the second shell of solvent for only Li^+ and Cs^+ ions. The notation is the same as in Fig. 2.

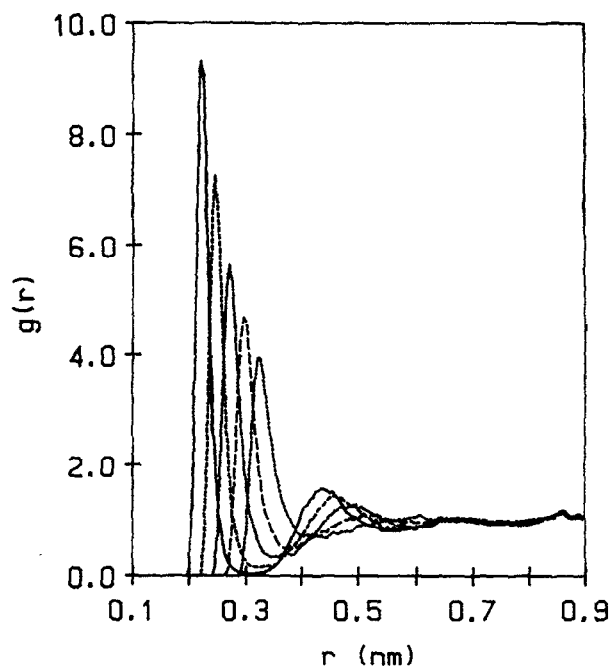


FIG. 5. Radial distribution functions g_{iw} of TIP4P water molecules as a function of the distance r_{iw} between the cation (i) and the center of mass of a water molecule (w). The notation is the same as in Fig. 2.

with increase in cation size thus implying again a weakening of the cation-water interaction. The first hydration shell is sharply defined for Li^+ within a narrow range of r , while it is broader for Cs^+ which has a lower maximum in $g_{iw}(r)$ that

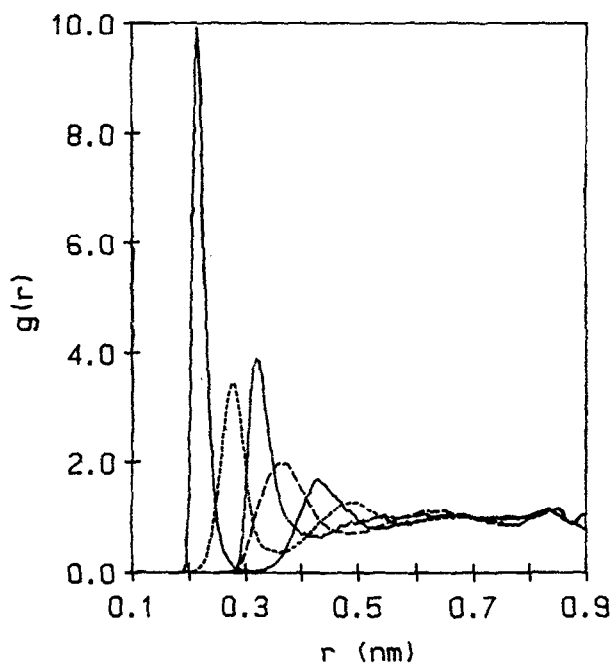


FIG. 6. The ion-oxygen g_{io} and ion-hydrogen g_{ih} radial distribution functions for Li^+ and Cs^+ ions: $g_{io}(r)$ (—) and $g_{ih}(r)$ (-----) for Li^+ ; $g_{io}(r)$ (---) and $g_{ih}(r)$ (---) for Cs^+ .

TABLE II. Positions and magnitudes at maxima and minima of ion-water radial distribution functions g_{iw} and water-water radial distribution functions g_{ww} in pure water at 25 °C.

Ion	First max		First min		Second max		Second min	
	r_{iw} (Å)	g_{iw}	r_{iw} (Å)	g_{iw}	r_{iw} (Å)	g_{iw}	r_{iw} (Å)	g_{iw}
Li ⁺	2.20	9.56	3.10	0.03	4.35	1.65	5.45	0.80
Na ⁺	2.45	7.00	3.50	0.22	4.70	1.38	5.65	0.81
K ⁺	2.70	5.64	3.65	0.35	4.95	1.30	5.80	0.88
Rb ⁺	2.95	4.68	3.90	0.51	5.15	1.11	(6.2) ^a	(0.91)
Cs ⁺	3.25	3.90	4.20	0.65	(6.1) ^a	(1.07)	(6.8) ^a	(0.93)
Water	r_{ww} (Å)	g_{ww}	r_{ww} (Å)	g_{ww}	r_{ww} (Å)	g_{ww}	r_{ww} (Å)	g_{ww}
H ₂ O	2.75	2.78	3.45	0.90	4.40	1.06	5.65	0.93

^aThe values in parenthesis are less accurately known than the others. The subscript w refers to the center of mass of the water molecule.

is shifted further away from the ion. There is also a pronounced second solvation shell around Li⁺, but the peak associated with this is less prominent for Na⁺ and K⁺. Only traces of the second shell remain for Rb⁺ and Cs⁺.

Figure 6 shows the ion-oxygen $g_{io}(r)$ and ion-hydrogen $g_{ih}(r)$ radial distribution functions for Li⁺ and Cs⁺ ions which lead to the same conclusions. Again, the cation-water radial distribution functions are essentially unaltered by an electric field of 1.0 V/nm. Table II contains the positions and magnitudes of the maxima and minima of $g_{iw}(r)$ in the first and second shells together with the corresponding values for the center-of-mass distribution functions $g_{ww}(r)$ in pure water at 25 °C.

The coordination number in the first shell around an ion, defined as the number of water molecules in that shell, is determined by integrating $g_{iw}(r)4\pi r^2 dr$ from $r=0$ up to the first minimum of $g_{iw}(r)$ beyond the origin. Table III displays the average coordination numbers in the primary shell of the cations, calculated from our simulations without and with an electric field of 1.0 V/nm. Although the electrostatic ion-water interaction decreases with ion size, the coordination numbers become larger with the accompanying increase in volume of the first shell. In Sec. III B we discuss how these numbers may change with time; the average values are, however, relatively insensitive to the applied electric field. Coordination numbers defined by using the ion-oxygen distribution functions $g_{io}(r)$ instead of $g_{iw}(r)$, would lead to numbers that are only slightly different from those reported here.

Figure 7 shows $h(r) = \mu \cdot \mathbf{r} / (|\mu||\mathbf{r}|)$ as a function of $r = |\mathbf{r}|$ for the free field case. Here \mathbf{r} is the cation-oxygen vector and

TABLE III. Average coordination number of water molecules around each cation without and with an electric field of 1.0 V/nm. The numbers in the second shell for Li⁺ and Cs⁺ are 17.5 ± 0.5 and 32.4 ± 0.5 , respectively.

Ion	0.0 V/nm	1.0 V/nm
Li ⁺	6.0 ± 0.1	6.0 ± 0.1
Na ⁺	6.6 ± 0.1	6.6 ± 0.1
K ⁺	8.0 ± 0.1	7.9 ± 0.3
Rb ⁺	8.9 ± 0.3	9.1 ± 0.1
Cs ⁺	10.0 ± 0.3	9.6 ± 0.4

μ is the water dipole vector. The larger values of $h(r)$ in the first shell of the smaller cations imply that these two vectors are more nearly parallel in the first shell when the ions are small. The traces of $h(r)$ remaining after its rapid decrease before the second shell indicate a weaker cation field at this distance and possible disruption of water due to hydrogen bonding between the first and second shell waters. However, the decay to zero at $r=0.65$ nm, followed by a slow increase, and rapid change to negative values remains unexplained except perhaps to indicate the formation and disruption

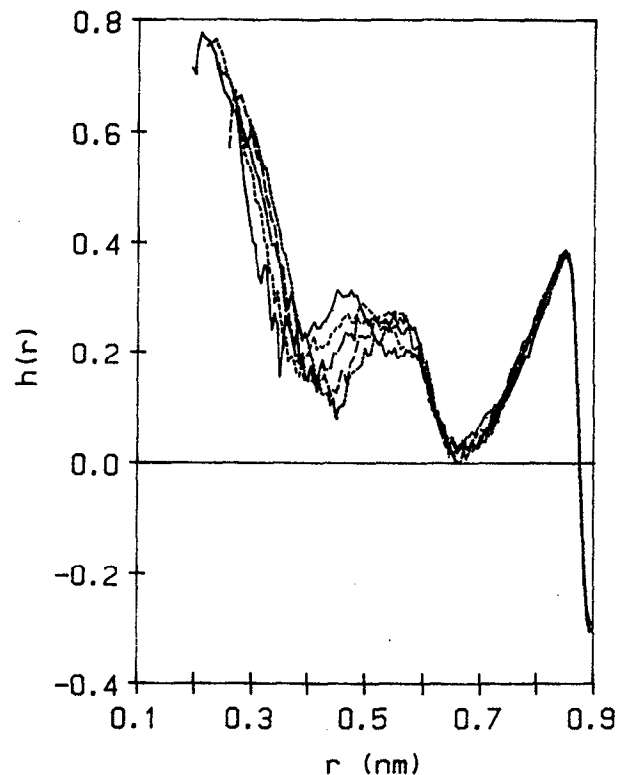


FIG. 7. The function $h(r) = \mu \cdot \mathbf{r} / (|\mu||\mathbf{r}|)$, where $r = |\mathbf{r}|$ is the cation-oxygen vector and μ is the water dipole vector plotted against r for different cations in the absence of an external electric field. The notation is the same as in Fig. 2.

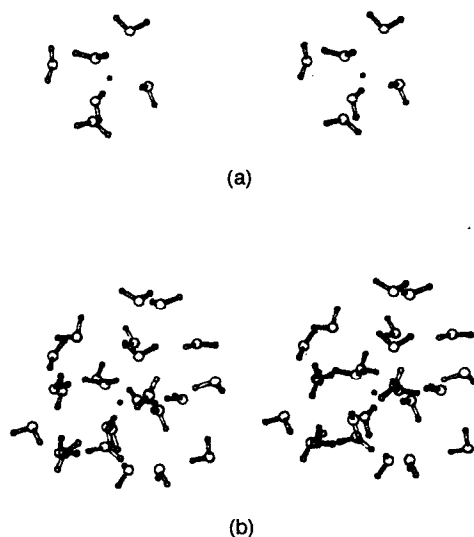


FIG. 8. Stereoscopic pictures of equilibrium configurations of TIP4P water molecules around Li^+ in (a) first (6 water molecules) and (b) first and second hydration shells (25 water molecules), respectively.

tion of water structure further away from the cation. We also note that the $h(r)$ functions (not shown) in the presence of an electric field of 1.0 V/nm are essentially the same as the functions without it.

In Figs. 8(a) and 8(b) we display stereoscopic pictures of equilibrium configurations of water in the first solvation shell alone and in the first and second solvation shells of Li^+ . Figure 9 shows a corresponding set of pictures for water molecules around Cs^+ . While the oxygen atoms of each water molecule in the first shell of Li^+ are closer to the ion than the hydrogens, it is remarkable that only three of six water dipoles appear to be pointed towards the Li^+ ion suggesting

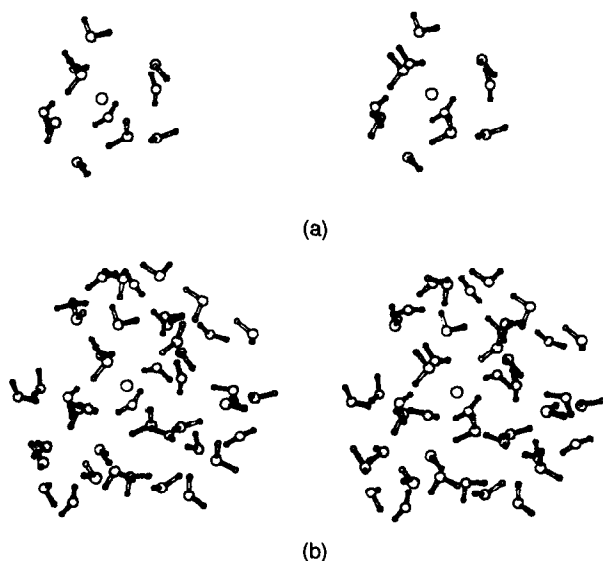


FIG. 9. Stereoscopic pictures of equilibrium configurations of TIP4P water molecules around Cs^+ in (a) first (11 water molecules) and (b) first and second hydration shells (43 water molecules), respectively.

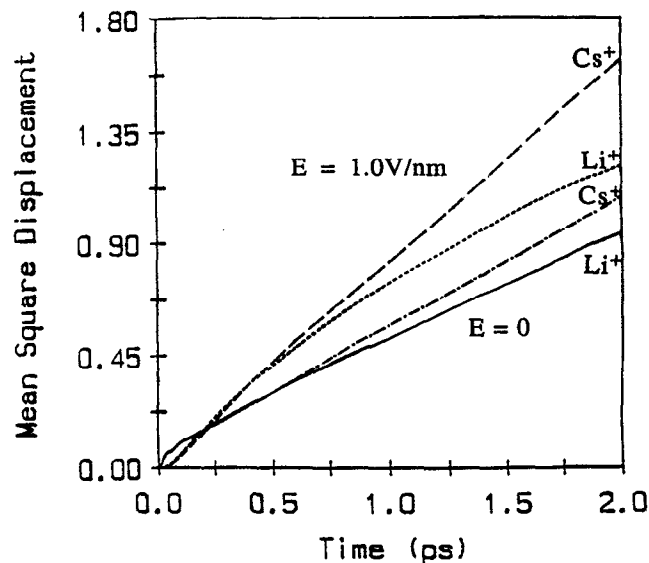


FIG. 10. Mean-square displacements in the units of 10^{-2} nm^2 for (i) Li^+ , at zero field $E=0$ (—) and $E=1.0$ V/nm (---) and for (ii) Cs^+ at zero field $E=0$ (---) and $E=1.0$ V/nm (---).

that there is considerable rotational motion of water in this shell. In the case of Cs^+ none of the first shell water dipoles points towards the ion in the equilibrium configuration shown, and the water molecules in the second layer also do not show any discernible structure. These pictures lend some support to the early ideas of Gurney⁴² and Frank and Evans⁴³ on the effect of ions on water structure, although they describe the behavior of only a particular model of water around these ions.

B. Dynamic properties

The velocity (VAC) and force autocorrelation (FAC) functions of the cations calculated without and with the electric field of 1.0 V/nm at 298 K are not shown, because we do not find any essential changes caused by the field. We used the Einstein relation⁴⁴

$$D = \frac{1}{6} \lim_{t \rightarrow \infty} d \langle |\mathbf{r}(t) - \mathbf{r}(0)|^2 \rangle / dt \quad (7)$$

to determine the diffusion coefficients D of the cations from the mean-square displacement (MSD) of the ions in the ab-

TABLE IV. Diffusion coefficient D calculated from the mean-square displacements (MSD) and velocity autocorrelation (VAC) functions in the absence of an electric field.

Ion	Diffusion coefficients	
	MSD	($10^{-5} \text{ cm}^2/\text{s}$) VAC
Li^+	0.66 ± 0.18	0.64 ± 0.18
Na^+	0.78 ± 0.13	0.70 ± 0.20
K^+	0.84 ± 0.28	0.83 ± 0.18
Rb^+	1.06 ± 0.14	1.04 ± 0.20
Cs^+	0.83 ± 0.12	0.82 ± 0.21

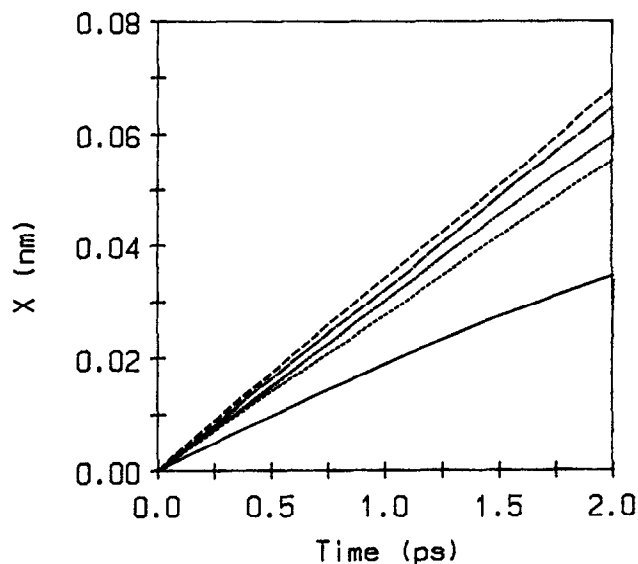


FIG. 11. The distances traveled by cations along the direction of an electric field of 1.0 V/nm. The notation is the same as in Fig. 2.

sence of an applied electric field. Figure 10 shows least squares fits to the MSD's calculated in our simulations for times close to 2 ps and Table IV provides the corresponding values of D . Our calculated D for Na^+ ($0.78 \pm 0.13 \times 10^{-5} \text{ cm}^2/\text{s}$) is slightly higher than Berkowitz and Wan's estimate²³ of $0.67 \pm 0.05 \times 10^{-5} \text{ cm}^2/\text{s}$, from the velocity autocorrelation function for this ion in the same model solvent. Less significantly perhaps, it is marginally closer to the experimental value at 25 °C of $1.33 \times 10^{-5} \text{ cm}^2/\text{s}$ for Na^+ at infinite dilution. The mean-square displacement increases upon applying an electric field, as seen in Fig. 10, in contrast to the insensitivity of the velocity and force autocorrelation functions and the static properties to the applied field. We will discuss this later.

The electric field determines the average drift velocities of the cations and the distances traveled by them. Constant drift velocities were observed in our simulations. Figure 11 shows that the distances traveled by the ions are almost linear functions of time at a constant field (1.0 V/nm), which implies that the frictional forces due to the cation-water interactions are nearly balanced by the external driving force.

TABLE V. Ionic mobilities ($10^{-4} \text{ cm}^2/\text{Vs}$) calculated from (1) the drift velocity and (2) the distances traveled by the cations in the presence of an applied field of 1.0 V/nm, (3) the MSD, and (4) the VAC functions of the cations in the absence of a field.

Ion	Cation Mobility calculated from			
	Drift velocity ($E = 1.0 \text{ V/nm}$)	Distance traveled	MSD	VAC
Li^+	1.80 ± 0.41	1.74 ± 0.29	2.56 ± 0.70	2.49 ± 0.70
Na^+	2.75 ± 0.30	2.76 ± 0.31	3.04 ± 0.50	2.72 ± 0.77
K^+	3.08 ± 0.54	3.23 ± 0.47	3.29 ± 1.09	3.23 ± 0.70
Rb^+	3.36 ± 0.39	3.37 ± 0.36	4.13 ± 0.54	4.05 ± 0.77
Cs^+	2.90 ± 0.40	3.01 ± 0.31	3.21 ± 0.46	3.19 ± 0.82

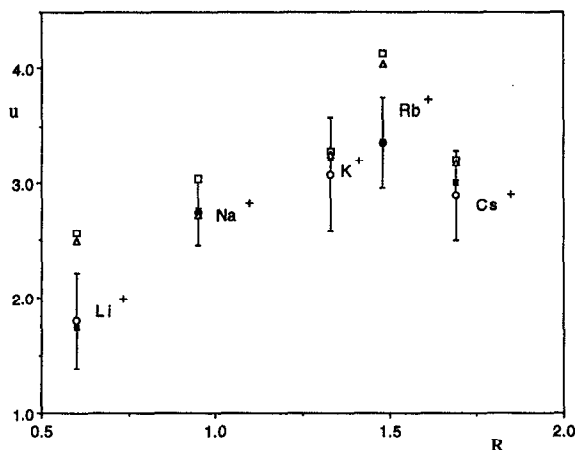


FIG. 12. Ion mobilities in units of $10^{-4} \text{ cm}^2/\text{Vs}$ as a function of the crystallographic radius R calculated from the average drift velocities (O) and the distances traveled (*) in the presence of an electric field $E = 1.0 \text{ V/nm}$ and from the mean-square displacement (\square) and the velocity autocorrelation function in the absence of an electric field (Δ). Only the error bars for mobilities computed from the drift velocities are shown; for the rest see Table V.

The drift velocity v determines the ionic mobility, since $u = v/E$, where E is the electric field and the limiting ionic conductance follows from the relation $\lambda = uF$.^{1(b),26} The mobility was also calculated from a least squares fit of the distance traveled by the ion as a function of time (see Fig. 11). Table V displays the calculated mobilities and Fig. 12 shows plots of the mobility as a function of the crystallographic radius of the cations. The two sets of results for u , from the drift velocities and the distances traveled by the cations, are in good agreement but they are approximately one-half the experimental values in real water.^{1(b),26} Their dependence on ion size is similar to the experimental mobilities depicted in Fig. 1. The mobility of Na^+ , calculated by us, agrees well with the simulations of Rose and Benjamin,²⁵ who also used an electric field in their simulations. They estimated $2.6 \pm 0.7 \times 10^{-4} \text{ cm}^2/\text{Vs}$ for the mobility of the sodium ion, compared to our calculation of $2.75 \pm 0.30 \times 10^{-4} \text{ cm}^2/\text{Vs}$.

We now return to the MSD in the presence of an electric field. If $\mathbf{r}(t)$ and $\mathbf{r}_0(t)$ are the respective positions of the ion in the presence and absence of a field, and v_z is the drift velocity in the z direction, we have

$$\mathbf{r}(t) = \mathbf{r}_0(t) + v_z t, \quad (8)$$

where the origin serves as the initial starting point at $t = 0$. We assume, for the sake of argument, that the drift velocity is attained instantaneously. Taking the dot product and ensemble average we have

$$\langle r(t)^2 \rangle = \langle r_0(t)^2 \rangle + 2 \langle r_{0,z}(t) \rangle v_z t + (v_z t)^2. \quad (9)$$

This shows that the two mean-square displacements are not the same even when $\langle r_{0,z}(t) \rangle$, the average displacement in the z direction at zero field, is zero. In this case, only the isotropic component of the MSD determines the diffusion coefficient D and it follows that Eq. (7) as it stands applies only when the field vanishes.

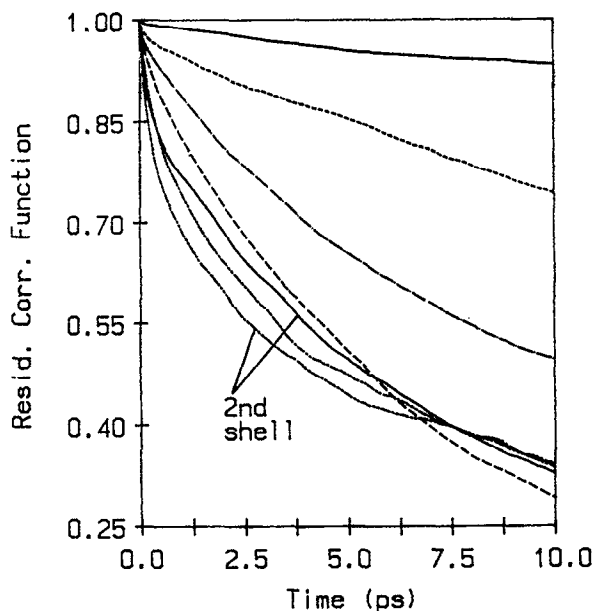


FIG. 13. Residence time correlation function for the hydrated TIP4P water molecules in the first hydration shell of each cation in the absence of an external electric field. The residence time correlation functions for Li^+ and Cs^+ in the second hydration shell are also shown. The notation is the same as in Fig. 2.

On the other hand, the velocity autocorrelation functions are insensitive to the fields used in our simulations since they are normalized by dividing by $\langle v(0)^2 \rangle$, where $v(0)$ is the appropriate field dependent initial velocity. Then, the diffusion coefficient calculated from the Kubo relation⁴⁴

$$D = \frac{1}{3kT} \int_0^\infty \langle \mathbf{v}(t) \cdot \mathbf{v}(0) \rangle dt \quad (10)$$

would also be field independent. Our calculations of the diffusion coefficient from the velocity autocorrelation functions are summarized in the second column of Table IV. The numbers presented are for $E=0$ and they agree very well with the diffusion coefficients determined from the mean square displacements in the absence of a field.

The diffusion and friction coefficients D and ζ are related by $D = kT/\zeta$, from which it follows that the mobility $u = Dq_i/kT$ since $u = q_i/\zeta$. This leads to independent estimates of the ion mobilities from the diffusion coefficients

TABLE VI. Characteristic decay times (ps) of hydrated water molecules in the first shell of each cation without and with an electric field of 1.0 V/nm. The decay times in the second shells of Li^+ and Cs^+ are 10.1 ± 1.0 and 12.3 ± 1.1 ps, respectively. For pure TIP4P water they are 5.34 ± 0.32 ps and 8.13 ps in the first and second shells, respectively.

Ion	0.0 V/nm	1.0 V/nm
Li^+	184 ± 57	203 ± 74
Na^+	37.6 ± 18.4	35.5 ± 10.0
K^+	14.9 ± 3.1	15.2 ± 4.9
Rb^+	8.4 ± 2.7	8.7 ± 1.5
Cs^+	11.1 ± 3.2	8.8 ± 2.2

determined in our simulations. The mobilities calculated, in this way, from the MSD and the VAC in the absence of a field are also displayed in Table V and are in excellent agreement for Na^+ , K^+ , and Cs^+ with those calculated from the drift velocities in the presence of a field. However, they are about 48% larger for Li^+ and Rb^+ than the drift velocity values; the errors in the mobilities from the diffusion coefficients are also nearly twice as large as the errors in the mobilities from the drift velocities. The agreement, however, is satisfactory considering the difficulty in obtaining good statistical averages for the diffusion coefficient of a single ion.

A major goal of this study is to try to understand the dependence of ionic mobility on the radius of the ion. We will focus our attention on the puzzle of the low mobility of a small cation in aqueous systems. To unravel this we consider the residence time correlation functions²¹ defined by

$$R(r,t) = \frac{1}{N_r} \sum_{i=1}^{N_r} [\theta(r,0)\theta(r,t)], \quad (11)$$

where $\theta(r,t)$ is the Heaviside unit step function that is 1 if a water molecule i is in a region r within a coordination shell of the ion and 0 otherwise, and N_r is the average number of water molecules in this region r at $t=0$. The $R(r,t)$ functions are determined by the strength of the solvation forces and their dynamics both in the presence of an electric field E and in its absence. Figure 13 shows the time dependence of $R(r,t)$, when $E=0$, for water in the first shell around Li^+ , Na^+ , K^+ , Rb^+ , and Cs^+ and for water in the second shell around Li^+ and Cs^+ . A characteristic decay time of the water in the shell at distance r from the ion is defined by

$$\tau = \int_0^\infty \langle R(r,t) \rangle dt. \quad (12)$$

Table VI shows the decay times in the first hydration shell obtained by fitting the time correlation function to an exponential decay $\langle R(r,t) \rangle \approx \exp(-t/\tau)$ which is especially useful when τ is large. Table VI also reveals the relatively small dependence of the decay time τ on the electric field.

The results of our simulations indicate that about 6.0 and 6.6 hydrated water molecules are kept in the first hydration shell around the Li^+ and Na^+ ions for nearly 190 and 35 ps, respectively, before significant exchange with the surrounding solvent and breakup of the solvation sheath occurs. The characteristic decay time of the solvation sheath for larger ions, which have 8–10 hydrated water molecules, decreases to about 8–11 ps. The residence times are generally insensitive to the external electric field. They are larger for small ions like Li^+ and Na^+ than the times reported by Impey *et al.*,²¹ which may be due to differences in the model parameters for water and ions. These calculations are reminiscent of the isotopic exchange experiments used to determine solvation times of inorganic aquocomplexes except that they are obtained directly by computer simulation for a model system.

The picture of the mobility of small cations that emerges from our studies is that of a hydrated “solventberg” ion, whose behavior is modulated by the decay of the solvent sheath immediately around the ion, and its interactions with

the surrounding water molecules which determine the dielectric friction. In the case of Li^+ , the number of hydrated water molecules in the first hydration shell remains nearly constant for about 190 ps, although exchange with the surroundings may take place during this time. The ion and its shell move together as an entity bestowing a large effective radius on the ion, on this time scale, and a small mobility. Indeed the ionic conductance of Li^+ is well approximated by Stokes law (see Fig. 1) if its radius is assumed to be the radius of the hydrated ion with its first shell of water molecules, i.e., 2.2 Å (see Table II). The water molecules in the first solvation shell are more weakly bound as the cation size increases, and they breakup and exchange with the surroundings at a faster rate. As we have seen, the coupling between the ion and the solvent is relatively insensitive to the external electric field used in our studies. Clearly, the solvation dynamics of the ions play a critical role in determining their mobilities in aqueous solutions.

IV. CONCLUDING REMARKS

We have carried out a series of molecular dynamics simulations of model cation-water systems where the cations are Li^+ , Na^+ , K^+ , Rb^+ , and Cs^+ . An analysis of the structural features shows that the strength of the cation-water electrostatic interaction becomes less important than the tendency of the water to maintain its structure and hydrogen-bonded network as the sizes of the cations increase. The maximum in the probability distribution function of the angle θ between the water-oxygen vector and the water dipole shifts from 22° to 52° , as the cation size increases. The structure of the surrounding water molecules around the cations and the dynamic properties, such as the VAC and FAC functions of the cations are unchanged on applying an external electric field. However, the mean-square displacements of the cations, their average velocities, and the distances traveled by them are affected by the field. The ionic mobilities calculated from the average velocities of the cations and the distances traveled in the presence of a field are in excellent agreement with each other and they are in satisfactory agreement with the mobilities determined from the mean-square displacement and the velocity autocorrelation function in the absence of a field. However, they underestimate the experimental values in real aqueous solutions but show the same dependence on ionic radii as the experimental ionic mobilities.

We conclude from our analysis of the residence time correlation functions of TIP4P water at 25 °C in the first solvation shell around the cations, that the hydrated water molecules around a Li^+ ion at infinite dilution are stuck to it for about 190 ps and move with it as an entity. For a Na^+ ion this time decreases to about 35 ps, while for the larger cations (Rb^+ and Cs^+) it is about 8 to 11 ps before significant exchange occurs with the surrounding solvent molecules. The concept of a solventberg ion whose low mobility is attributed to the large size of the solvated ion is well known.^{1,43,45} Our calculations support this picture of small ions in aqueous solution at room temperature over a time scale smaller than the characteristic decay time of the first solvation shell. The explanation of the behavior of ions

larger than Li^+ is more complicated, although our simulations suggest that linear response theory should provide an adequate basis for understanding the mobilities of these ions. Further studies on ionic mobilities in water and nonaqueous solvents, and their relationship to solvation dynamics, are in progress.

ACKNOWLEDGMENTS

This work was supported by Research Grant No. 911-0303-007-1 from the Korea Science and Engineering Foundation and by the Nondirected Research Fund of the Korea Research Foundation, 1992. S. H. L. thanks the Korea Institute of Sciences and Technology for access to the CRAY-2S and CRAY-C90 super computers and J. C. R. acknowledges the facilities provided by the Computer and Data Processing Services (CAPS) at the University of Maine.

- ¹(a) H. S. Frank, *Chemical Physics of Ionic Solutions* (Wiley, New York, 1956), p. 60; (b) R. A. Robinson and R. H. Stokes, *Electrolyte Solutions*, 2nd Ed. (Butterworth, London, 1959); (c) R. L. Kay, in *Water, A Comprehensive Treatise*, edited by F. Franks (Plenum, New York, 1973), Vol. 3.
- ²R. Lorenz, *Z. Phys. Chem.* **37**, 252 (1910).
- ³M. Born, *Z. Phys.* **1**, 221 (1920).
- ⁴R. M. Fuoss, *Proc. Natl. Acad. Sci.* **45**, 807 (1959).
- ⁵R. H. Boyd, *J. Chem. Phys.* **35**, 1281 (1961).
- ⁶R. Zwanzig, *J. Chem. Phys.* **38**, 1603 (1963); **52**, 3625 (1970).
- ⁷J. Hubbard and L. Onsager, *J. Chem. Phys.* **67**, 4850 (1977).
- ⁸J. Hubbard, *J. Chem. Phys.* **68**, 1649 (1978).
- ⁹J. Hubbard and R. F. Kayser, *J. Chem. Phys.* **74**, 3535 (1981).
- ¹⁰J. Hubbard and R. F. Kayser, *J. Chem. Phys.* **76**, 3377 (1982).
- ¹¹P. J. Stiles, J. Hubbard, and R. F. Kayser, *J. Chem. Phys.* **77**, 6189 (1982).
- ¹²N. Takisawa, J. Osugi, and M. Nakahara, *J. Phys. Chem.* **85**, 3582 (1981); M. Nakahara, T. Torok, N. Takisawa, and J. Osugi, *J. Chem. Phys.* **76**, 5145 (1982); N. Takisawa, J. Osugi, and M. Nakahara, *ibid.* **77**, 4717 (1982); **78**, 2591 (1983).
- ¹³H. G. Hertz, in *Water, A Comprehensive Treatise*, edited by F. Franks (Plenum, New York, 1973), Vol. 3.
- ¹⁴P. G. Wolynes, *J. Chem. Phys.* **68**, 473 (1978); P. Colonosmos and P. G. Wolynes, *J. Chem. Phys.* **71**, 2644 (1979).
- ¹⁵P. Wolynes, *Ann. Rev. Phys. Chem.* **31**, 345 (1980); J. Hubbard and P. Wolynes, in *Theories of Solvated Ion Dynamics*, Chap. 1 of *The Chemical Physics of Ion Solvation, Part C*, edited by R. R. Dogonadze, E. Kalman, A. A. Kornyshev, and J. Ulstrup (Elsevier, New York, 1985); in *Non-Equilibrium Theories of Electrolyte Solutions of The Physics and Chemistry of Aqueous Ionic Solutions*, edited by M. C. Bellissent-Funel and G. W. Neilson (Reidel, Dordrecht, 1987).
- ¹⁶G. Ciccotti and G. Jacucci, *Phys. Rev. Lett.* **35**, 789 (1975).
- ¹⁷E. M. Gosling and K. Singer, *Chem. Phys. Lett.* **39**, 361 (1976).
- ¹⁸E. L. Pollock and B. J. Alder, *Phys. Rev. Lett.* **41**, 903 (1978).
- ¹⁹M. Mezei and D. L. Beveridge, *J. Chem. Phys.* **74**, 6903 (1981).
- ²⁰H. L. Nguyen and S. A. Adelman, *J. Chem. Phys.* **81**, 4564 (1984).
- ²¹R. W. Impey, P. A. Madden, and I. R. McDonald, *J. Chem. Phys.* **87**, 5071 (1985).
- ²²M. A. Wilson, A. Pohorille, and L. R. Pratt, *J. Chem. Phys.* **83**, 5832 (1985).
- ²³M. Berkowitz and W. Wan, *J. Chem. Phys.* **86**, 376 (1987).
- ²⁴M. R. Reddy and M. Berkowitz, *J. Chem. Phys.* **88**, 7104 (1988).
- ²⁵D. A. Rose and I. Benjamin, *J. Chem. Phys.* **98**, 2283 (1993).
- ²⁶P. W. Atkins, *Physical Chemistry*, 4th ed. (Freeman, San Francisco, 1990), pp. 755–756 and 963.
- ²⁷D. R. Lide, *Handbook of Chemistry and Physics*, 71st ed. (CRC, Boca Raton, FL, 1990), pp. 5–97.
- ²⁸L. Perera and M. Berkowitz, *J. Chem. Phys.* **96**, 3092 (1992); in *Solvation Dynamics in a Stockmayer Fluid*, in *Condensed Matter Theories*, edited by L. Blum and F. B. Malik (Plenum, New York, 1993), Vol. 8.
- ²⁹E. Neria and A. Nitzan, *J. Chem. Phys.* **96**, 5433 (1992); E. Neria and A. Nitzan, in *Numerical Studies of Solvation Dynamics in Electrolyte Solutions*, in *Ultrafast Reaction Dynamics and Solvent Effects*, AIP Conf. Proc. No. 298, edited by Y. Gaudel and P. Rossky (AIP, New York, 1993).

- ³⁰M. Maroncelli, P. V. Kumar, A. Papazyan, M. Hornig, S. J. Rosenthal and G. R. Fleming, in *Ultrafast Reaction Dynamics and Solvent Effects*, AIP Conf. Proc. No. 298, edited by Y. Gauduel and P. Rossky (AIP, New York, 1993), and references therein.
- ³¹S. H. Lee, J. C. Rasaiah, and J. Hubbard, *J. Chem. Phys.* **85**, 5232 (1986); **86**, 2383 (1987).
- ³²W. L. Jorgenson, J. W. Madura, R. W. Impey, and M. L. Klein, *J. Chem. Phys.* **79**, 926 (1983).
- ³³J. Chandrasekhar, D. Spellmeyer, and W. L. Jorgensen, *J. Am. Chem. Soc.* **106**, 903 (1984).
- ³⁴W. L. Jorgensen, *J. Chem. Phys.* **77**, 4156 (1982).
- ³⁵G. Y. Szasz and K. Heinzinger, *Z. Naturforsch.* **38a**, 214 (1983).
- ³⁶O. Steinhäuser, *Mol. Phys.* **45**, 335 (1982).
- ³⁷K. F. Gauss and J. Reine, *Angev. Math.* **IV**, 232 (1829).
- ³⁸W. G. Hoover, A. J. C. Ladd, and B. Moran, *Phys. Rev. Lett.* **48**, 1818 (1982).
- ³⁹D. J. Evans, *J. Chem. Phys.* **78**, 3297 (1983).
- ⁴⁰D. J. Evans, *Mol. Phys.* **34**, 317 (1977); D. J. Evans and S. Murad, *ibid.* **34**, 327 (1977).
- ⁴¹W. C. Gear, *Numerical Initial Value Problems in Ordinary Differential Equations* (McGraw-Hill, New York, 1965).
- ⁴²H. S. Frank and M. W. Evans, *J. Chem. Phys.* **13**, 507 (1945).
- ⁴³R. W. Gurney, *Ions in Solution* (Dover, New York, 1962); *Ionic Processes in Solution* (Dover, New York, 1962).
- ⁴⁴D. A. McQuarrie, *Statistical Mechanics* (Harper and Row, New York, 1976).
- ⁴⁵R. S. Berry, S. A. Rice, and J. Ross, *Physical Chemistry* (Wiley, New York, 1980), p. 422.